Mold filling stability analysis for metal compounds

Stevenson, J.; Ilinca, Florin

ANTEC 2004 : conference proceedings, 2004

IMI2004-103081-G
CNRC 46835

MOLD FILLING STABILITY ANALYSIS FOR METAL COMPOUNDS

James F. Stevenson, Honeywell International, Morristown, New Jersey 07962
Florin Ilinca, National Research Council of Canada, Boucherville, Quebec J4B6Y4

Abstract

Metal injection molding (MIM) is similar to plastic molding in many respects, but compounds (metal powders with polymer binders) are more susceptible to thermally induced flow instability because of their higher thermal diffusivity. Stable and unstable (asymmetric) flow patterns for a stainless steel MIM compound were observed and accurately simulated for filling through a diaphragm gate over a range of fill times and melt/mold temperatures. Simulation predicted the observed free annular jet and internal voids in the molded part. For unstable flow, an exponential increase in temperature differences at symmetric locations was predicted during mold filling. Based on observation and simulation, a boundary was established between regions of stable and unstable flow in terms of the dimensionless Graetz number Gz (ratio of heat conduction time to fill time) and B, a dimensionless ratio indicating viscosity sensitivity to temperature differences in the mold.

Introduction

A flowing fluid that is cooled has the potential for a thermally induced instability. A small local decrease in temperature will cause an increase in viscosity that will in turn decrease flow. For a fluid that has cooled sufficiently, these changes will cascade until the flow virtually ceases in one region and accelerates in adjacent regions.

This work is a more comprehensive analysis of our prior publications on the flow geometry in Figs. 1 and 2 (1,2,3). Previously Shaw and Pearson (4) analyzed the stability of polymer flow for a power-law fluid in a radial geometry. Their results generally predict unstable flow above a critical dimensionless temperature difference B and low Gz with the stability boundary along a line of B proportional to Gz with increasing Gz.

Molding

The material used here was a commercial molding compound, PowderFlo® 17-4PH U, composed of gas-atomized 17-4 stainless steel powder in an aqueous-gel binder. The rheological properties of this material were characterized by Datapoint in Ithaca, NY and are summarized in Table 2.

The MIM compound was processed on a 55-ton Cincinnati Milacron injection molding machine with a 28-mm low compression screw. The mold was a thick-walled M-shaped block with a central hole as shown in Fig 2(a) as a finite element mesh. The mold cavity (volume = 30 cm^3) was filled through a diaphragm gate on the lower surface. The gate had an inner (sprue) / outer diameter ratio of 0.851 / 1.519 cm and thickness of 0.314 cm as shown in Fig. 2(c). The lower surface of the gate was a stainless steel bushing; the upper surface and mold walls were aluminum.

The filling of the M-mold cavity was investigated for the following combinations of inlet melt/mold coolant temperatures: A: 82/12°C, B: 71/15°C, C: 82/15°C, and D: 82/27°C. For each set of temperatures, successive short shots showing the fill pattern were obtained at nominal fill times of 2 and 8 sec. Short shots at a fixed fractional fill were made over a range of fill times to identify stable and unstable filling conditions.

Governing Equations

The governing equations for the simulation are the conservation relations for momentum, energy, and mass for an incompressible fluid with the Modified Cross viscosity model given in Table 2 (1-3). These equations were cast in dimensionless form; the characteristic variables (indicated by '), dimensionless variables (indicated by *) and resulting dimensionless numbers are given in Table 1. Dimensionless groups given in Table 1 that appear in the governing equations or locations on the boundary conditions are Gz, B, Br, R/H, r^*_{inlet}, and rheological parameters. These groups could influence the location of the stability line and are discussed here and in the Stability Diagram section.

The dimensionless Graetz number Gz is the ratio of a characteristic time for heat condition to the time for heat transport by convention (flow). Small Gz (thin channels, slow flow, long flow path) means there is time for substantial cooling of the flowing material.

The characteristic temperature for viscosity ΔT_{rheol} is the temperature increase that is needed for a decrease in the predicted viscosity by a factor of 2.72, the base for natural logarithms. In this paper, ΔT_{rheol} is evaluated at the characteristic shear rate γ and T_{av} the average of the inlet and wall temperatures. A low value of ΔT_{rheol} indicates high temperature dependence for the viscosity.

B is the ratio of the operating temperature difference $T_{inlet} - T_{wall}$ to ΔT_{rheol}. A large value for B means the combination of the temperature sensitivity of viscosity and operating temperature differences will result in a large change in viscosity if the flowing material has sufficient time to cool (small Gz). In cases where B has two values (e.g. two mold wall temperatures), the higher value was used since instability at one wall will tend to propagate.

Simulation

Filling of the M-shaped tool and the two gate geometries, all shown in Fig. 2, was simulated using a 3D finite element code developed by the National Research Council of Canada. This code is described in previous publications (1-3).

The mesh for the mold, shown in Fig. 2, contains 92,569 nodes and 516,240 tetrahedral elements. Computations, typically requiring 48 hours, were carried out on an SGI Origin 2000 parallel computer using six processors.

Nonslip boundary conditions were applied to the cavity walls in filled regions and a zero shear stress condition was specified on the free surface. Heat transfer between the melt-mold interface and the mold interior was modeled by the expression

$$q_m = h_c(T_{wall}-T_m) \qquad (1)$$

q_m is the heat flux at the mold wall, h_c is the surface heat transfer coefficient, T_{wall} is the temperature at the melt-wall interface and T_m is the temperature of the coolant.

For computations for the M-cavity, the viscosity model included a yield stress (1-3). The yield stress was observed to have little influence on the flow pattern and did not change the stable/unstable nature of the flow.

Computations showing stable and unstable filling of the M-shaped mold are given in previous publications (1-3). Generally these simulations predict the shape of an annular jet formed by the material exiting from the gate. Both steady flow and severely asymmetric unsteady flow are predicted depending on thermal and flow conditions. Both experiment and simulation show that a thicker gate reduces the tendency to form an annular jet and the resulting interior and surface defects due to trapped air (3). The gate geometry for these simulations is correct (1-3) but the mold volume was erroneously only 60% of the actual mold volume.

For the diaphragm gate (Fig. 2(c)) with the same dimensions as the mold gate, the build up of differences between the maximum and minimum temperatures at the + and - exit locations (Fig. 1) is shown in Fig. 3. For the fast fill times (2-4 sec), the temperature difference builds up to a plateau value of less than 10^{-3}°C. For the 8-sec fill, the temperature difference increases exponentially but at a sufficiently slow rate so that an observable instability would not occur during mold filling. For the 16 and 32-sec fill times, the build up of the temperature instability results in a temperature difference exceeding 30°C and unstable, asymmetric flow.

Stability Diagram

More than 60 simulations and 34 experimental observations of stable, transition, and unstable flow were used to prepare diagrams with dimensionless numbers as coordinates to identify regions of stable and unstable flow.

For both simulations and experiment, the wall temperature T_{wall} was estimated by equating an expression for the heat flux through the part (given by an assumed linear temperature gradient) to the heat flux at the mold wall in terms of the heat transfer coefficient (HTC).

$$T_{wall} = T_m + (T_{inlet} - T_m)/(1 + h_c H / k_{MIM}) \qquad (2)$$

where k_{MIM} is the thermal conductivity of the MIM compound. T_{wall} typically ranged from 2 to 6°C above the coolant temperature for high values of the heat transfer coefficient (100,000 W/m^2-K) up to 36°C for the standard value of 4000 W/m^2-K. A HTC of 4000 W/m^2-K was used to estimate T_{wall} for the experimental data. This value corresponds to steady heat transfer over a distance in an aluminum mold of 5.2 cm. For the M mold geometry, this is a reasonable distance, but the transient nature of heat transfer for material first entering the mold is not considered.

Stability for the molded samples was judged by the symmetry of the short shot; asymmetry was generally considered unstable; unless it was slight, in which case, it was labeled transitional. Simulated flow was considered stable if the temperature differences approached low plateau values, generally < 10^{-1} °C (maximum allowed is 0.3°C), during mold filling prior to contacting the outside wall. High plateau values for the temperature difference, > 10 °C, indicate unstable flow.

Points indicating stable (filled symbols) and unstable flow (open symbols) for simulation are plotted in Fig. 4 on B vs. Gz axes. The simulated runs were generally for fixed values of the mold and inlet melt temperatures with a range of fill times. In the legend of Fig. 4 for simulation, the first number is the case number and the second number corresponds to a particular inlet and mold temperature combination. Cases 1-24 are for filling the M-mold; the remaining cases up to 66 are for the gate only. Tables summarizing cases are available from the authors. The experimental data obtained from four sets of temperature conditions are also plotted in Fig. 4 as shadowed squares having internal characters denoting stable flow and shadowed characters alone (x,+,*) indicating unstable flow. Series A had only one point which was stable. Transition is indicated by squares with internal yellow characters.

The data points in Fig. 4 generally separate into

(a) a region of stable flow which corresponds to a combination of relatively high flow rates in thick gates (large Gz) and small change in viscosity due to temperature change during flow (low B), and

(b) a region of unstable flow caused by viscosity increases due to large temperature drops associated with relatively slow filling in thin parts with a large temperature difference between the entering melt and a mold wall.

As Gz becomes very small (long fill times), the line separating stable and unstable regions appears to approach a limiting value for B below which the flow is stable regardless of fill time. The existence of this asymptote was predicted by Shah and Pearson (4).

Other dimensionless groups given in Table 1, Br, R/H, and r^*_{inlet} could also influence the location of the stability line. These groups are either not significant because of magnitude (Br<<1) or shown by inspection not to influence the stability results in Fig. 4 (3). Material rheology was not a variable in this work since all moldings and simulations were done with the same material. Previous work (4) has shown the power-law index n to be a significant variable.

The common experience of unexpectedly molding defective parts following a long run of good parts may be explained by operating too close to the stability boundary. In this case, the solution is to move toward the more stable region by increasing injection speed or coolant temperatures, or decreasing the barrel temperature set points.

Acknowledgments

The authors wish to acknowledge National Research Council of Canada for continuing support of the computational portion of this work and Honeywell International for sponsoring the molding trials. We wish to acknowledge Gary Marsh of Honeywell and Brian Holmes of Columbia Plastics for molding operations.

References

1. Ilinca, F., Hetu, J.-F., Derdouri, A., Holmes, B., Scott, C., and Stevenson, J. F., "Simulation of Metal Injection Molding: Three Dimensional Flow with Inertia and Free Surface Boundary Conditions," *SPE ANTEC Proceedings*, 58, 718-722 (2000).

2. Ilinca, F., Hetu, J.-F., Derdouri, A. and Stevenson, J. F. "Metal Injection Mold Molding: 3D Modeling of Non-isothermal Filling," *Polym. Eng. Sci.*, 42, 760 (2002).

3. Stevenson, J. F., Ilinca, F., "Thermally Induced Flow Instability In Metal Injection Molding," *Advances in Powder Metallurgy & Particulate Materials*, 8-110 (2003).

4. Shah, Y. T., and Pearson, J. R. A., "Stability of Non-isothermal Flow in Channels--II. Temperature Dependent Power-Law Fluids without Heat Generation," *Chem. Engng. Sci*, 29, 737-746 (1974), --III. Temperature Dependent Power-Law Fluids with Heat Generation," *Chem. Engng. Sci*, 29, 1485-1493 (1974).

Key Words: stability, unstable, metal injection molding, flow, temperature, simulation,

Table 1. Summary of Characteristic Variables and Dimensionless Variables and Numbers.

Variable, Symbol	Characteristic Variable	Definition	Dimensionless Variable
Coordinates, axial z, radial r	H	Half height	$z^* = z/H$, $r^* = r/H$
Time, t	t_{fill}	Fill time	$t^* = t/t_{fill}$
Temperature, T	T_{av}	Average temperature $T_{av} = (T_{inlet} + T_{wall})/2$	$T^* = (T - T_{wall})/(T_{inlet} - T_{wall})$
Pressure, p	p'	$= \eta' \gamma$	$p^* = p/\eta'\gamma$
Viscosity, η	η'	$= \eta_0/[1 + (\eta_0 \gamma/\tau)^{1-n}]$, $\eta_0 = \eta_0(T_{av})$	$\eta^* = \eta/\eta'$
Velocity, v	U	$= R/t_{fill}$	$v^* = v/U$
Shear Rate, γ	γ	$= U/H$	$\gamma^* = \gamma/(R/(t_{fill} H)$
Operating Temperature Change	ΔT_{op}	$= T_{inlet} - T_{wall}$	
Rheology Temperature Change	ΔT_{rheol}	$=[\lvert\partial \ln(\eta)/\partial T\rvert]^{-1}$ at T_{av} and γ	
Inlet radius, r_{inlet}	H	Inner radius of gate	$r_{inlet}^* = r_{inlet}/H$
Flow Length, R	H	Radial flow distance	R/H
Graetz Number		$= t_{cond}/t_{conv} = (\rho C_p H^2/k)/(R/U)$	Gz
Temperature Ratio		$= (T_{inlet} - T_{wall})/\Delta T_{rheol}$	B
Brinkman Number		$= \eta' U^2/[k(T_{inlet} - T_{wall})]$	Br

Table 2: Material Properties for 17-4 U Metal Powder.
Modified Cross-WLF Model: $\eta = \eta_0/[1 + (\eta_0 \gamma/\tau^*)^{1-n}]$
where $\eta_0 = \eta_{ref} \exp[-C_1(T - T_{ref})/(C_2 + T - T_{ref})]$ and $T_{ref} = D_2 + D_3 p$ and $C_2 = A_2 + D_3 p$

Material Properties		Cross / WLF and Yield Stress Model Constants					
Density (kg/m^3)	4887	n	0.206	D_2 (K)	273	A_2 (K)	51.60
Specific Heat (J/kg-K)	1001	τ^* (Pa)	2.487×10^4	D_3 (K/Pa)	0	τ_y (Pa)	10^4
Thermal Conductivity (W/m-K)	7.3	η_{ref} (Pa-s)	2.572×10^{19}	C_1 (-)	57.27	a (sec)	10^3

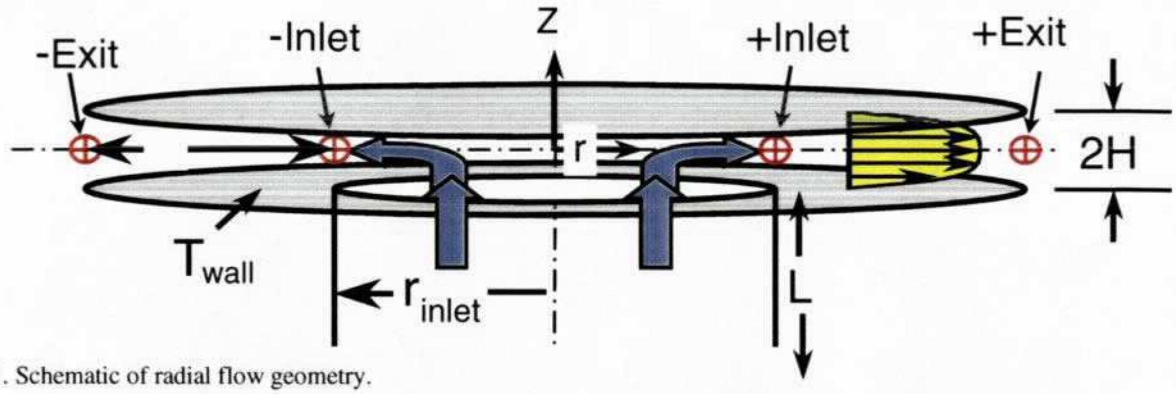

Fig. 1. Schematic of radial flow geometry.

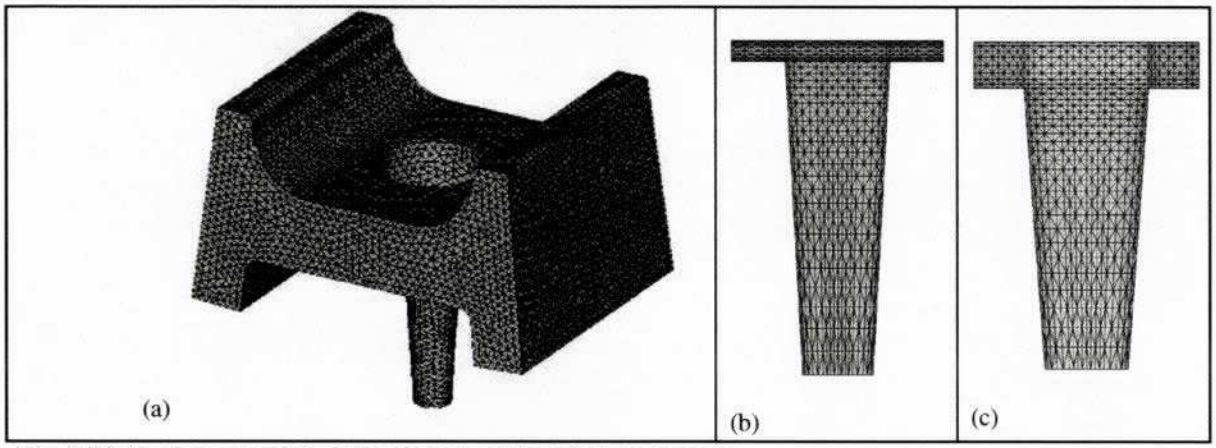

Fig. 2. Finite element mesh for M-body part and two diaphragm gates.

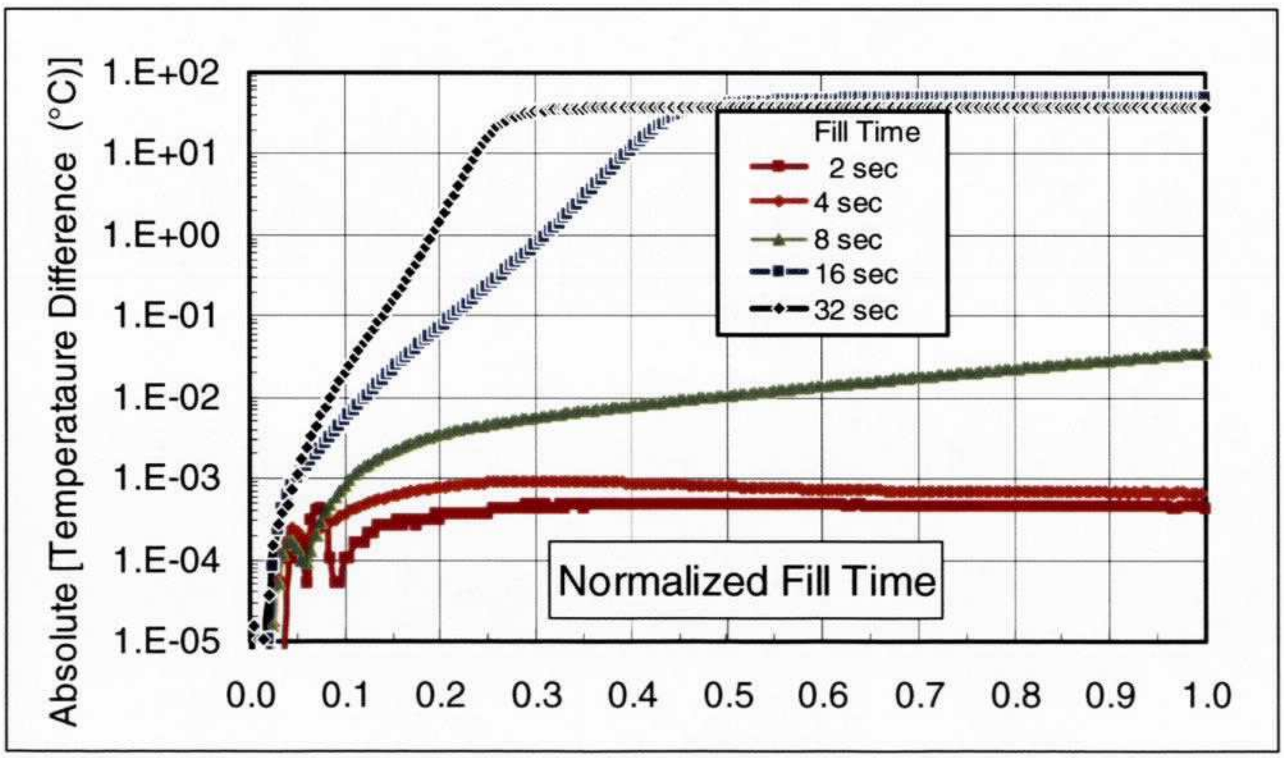

Fig. 3. Temperature differences predicted for flow through the thick diaphragm gate mold, cases 55-59. (3.14-mm gate, 30°C coolant temperature, 82°C inlet melt temperature)

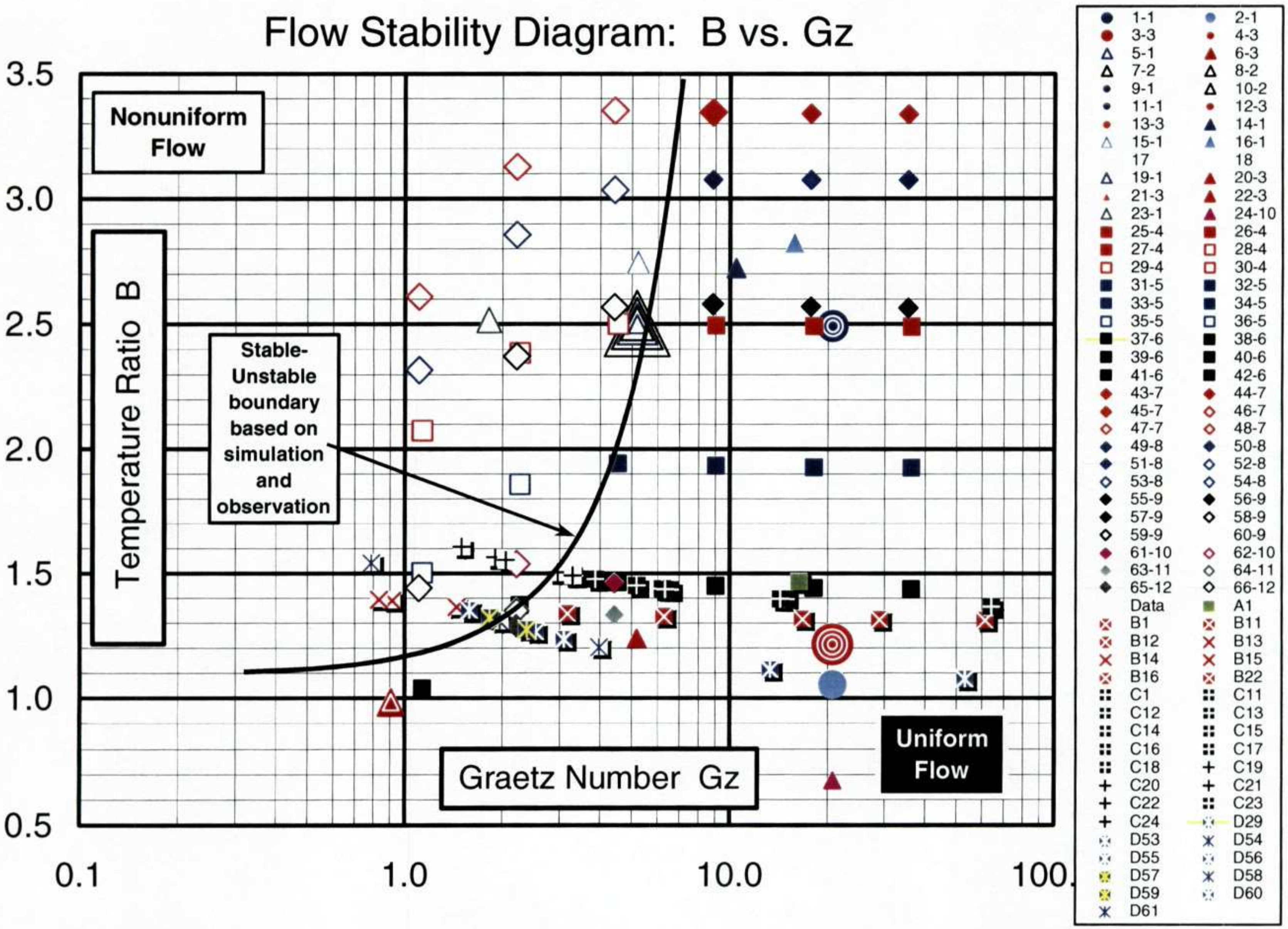

Fig. 4. Flow stability diagram of B vs. Gz based on experimental measurement and simulation.